

# Influence of process conditions on the surface oxidation of silicon nitride green compacts

S. M. CASTANHO\*, R. MORENO

*Instituto de Cerámica y Vidrio, CSIC, 28500 Arganda del Rey, Madrid, Spain*

J. L. G. FIERRO

*Instituto de Catálisis y Petroleoquímica, CSIC, Cantoblanco-28049 Madrid, Spain*

The surface chemistry of silicon nitride is strongly influenced by the processing environment. Mixing and forming steps can modify the oxidation state at the surface of the particle. The aim of the present investigation is to determine the possible changes and interactions on the surface of the particle induced during processing by different techniques of formation, such as isostatic pressing and slip casting. The effect of mixing conditions on surface oxidation have also been analysed on the green cast and pressed bodies prepared by dry and wet mixing using both water and alcohol as the mixing vehicles. X-ray photoelectron spectroscopy (XPS) has been used to characterize surface oxidation of the silicon nitride taking into account the Si2p, N1s and O1s binding energies, as well as the corresponding photoelectron line intensities. All processing treatments result in some surface oxidation. The Si2p peaks have two components in all studied conditions (due to nitride and oxynitride species) whereas N1s peaks are doublets for slip-cast samples and singlets in the pressed samples, thus suggesting a displacement of oxidized species by silica. In the case of slip-cast samples, the dispersant tetramethylammonium hydroxide (TMAH) seems to form a protective screen on the particles preventing further oxidation.

## 1. Introduction

Silicon nitride is of great interest for high temperature applications because of its high strength, high thermal-shock resistance and good wear resistance [1, 2]. It has been shown that high strength and good reliability can be achieved by careful processing of concentrated suspensions of silicon nitride powders. However, silicon nitride is strongly reactive and can be readily oxidized upon exposure to air [3, 4]. Oxidation of nitride thin films has been identified by Auger electron spectroscopy (AES) even at room temperature [5]. An XPS study by Raider *et al.* [4] of the oxidation of a silicon nitride film suggests that there is a rapid initial oxidation of its surface at room temperature upon exposure of the nitride film to air. Their data reveal that there is always some amount of oxygen in the film if the film is etched with hydrogen fluoride (HF). In line with this, several bulk chemical and surface analyses of oxygen distributions in various Si<sub>3</sub>N<sub>4</sub> powders manufactured by different processing techniques reveal significant differences in the oxygen contents at the surface of the particle. In order to understand the surface chemistry of Si<sub>3</sub>N<sub>4</sub> powders, some researchers have used pretreatment strategies trying to ensure that the properties in dispersions

reflect those of the powders in pristine states. These pretreatments do not always avoid possible oxidation from mixing, drying or formation processing steps.

The interfacial chemistry of ceramic powder dispersions is strongly related to the powder's casting rheological behaviour, the extent of inhomogeneities in the green body, and the physical properties of the final sintered product [5]. However, the influence of the chemical surface is not restricted only to casting processes since the different species formed on the Si<sub>3</sub>N<sub>4</sub> surface can affect the behaviour in different ways during densification and hence the properties of the final product.

This paper aims to present a more complete characterization of the silicon nitride surface region and how it behaves under different processes in order to evaluate the possible surface changes and interactions induced during formation by slip casting and isostatic pressing either in aqueous or in organic mixing vehicles. Both compositions and chemical states of the atoms at the surfaces generated during processing are evaluated by XPS. This information will be useful for engineering reliability, which is a key step for the development of ceramic applications.

\* Permanent address. IPEN-CNEN/SP CP054 222-970, São Paulo, Brasil.

## 2. Experimental procedure

A silicon nitride powder (LC12-SX) has been used as the starting material. The characteristics of the powder were supplied by the manufacturer and the specifications are summarized in Table I. The specific surface area of the material was calculated by the Brunauer–Emmett–Teller (BET) method from the nitrogen absorption isotherms measured at the temperature of liquid nitrogen. The particle size of the powder was determined using a laser particle size analyser (Coulter LS).

Two different techniques have been used in the present study for processing the original silicon nitride powder: (1) isostatic pressing, and (2) slip casting. For procedure 1 an initial mixing step of the  $\text{Si}_3\text{N}_4$  powder in a solvent is required. Isopropyl alcohol is usually employed as a liquid medium in attrition milling operations. The organic solvent should have a lower oxidation effect than water on the non-oxidic particle surface. However, the data reported in the literature are very confusing since there are no systematic studies comparing the effects of processing conditions on surface oxidation. In order to provide comparisons, three sets of isopressed samples were prepared:

1. the starting powder sample without any liquid,
2. homogenizing with water as the dispersant, and
3. homogenizing with isopropyl alcohol as the dispersant.

In cases 2 and 3 homogenizing was performed by attrition milling in a Teflon jar for 2 h. The homogenized powders were then dried and screened with a mesh below  $60\ \mu\text{m}$  and isopressed at 200 MPa. In procedure 2 (slip casting), a powder is dispersed in a liquid medium, which is responsible for the formation of a charged double layer around the particles. This double layer controls the electrochemistry of the system and thus the stability of the suspensions. Consequently, the chemistry at the surface is strongly dependent on the dispersing conditions, i.e. the solvent and the dispersant play key roles in the charge behaviour. Aqueous silicon nitride slips with solid loadings up to 65 wt % were prepared using TMAH as a dispersant. The slips were homogenized using a high speed mixer for 3 min. Bubbles were removed after 30 min low speed stirring. The final slips were cast on plaster moulds. Cast green bodies were dried in air for 24 h.

Cylindrical bars with 5 mm diameter were prepared for all formation procedures and conditions. The surface analyses were performed on fracture surfaces.

Photoelectron spectra were obtained using a Fisons ESCALAB MkII electron spectrometer employing  $\text{MgK}_\alpha$  X-rays (photon energy,  $h\nu = 1253.6\ \text{eV}$ ), and an

electron take-off angle of  $45^\circ$ . The base pressure of the spectrometer was typically  $10^{-7}\ \text{Pa}$ . The X-ray gun was operated at 12 kV and 10 mA, corresponding to a power of 120 W. A survey spectrum (50–1150 eV) was recorded for each sample (single scan) followed by Si2p, N1s, O1s and C1s regions where appropriate (60 scans). The analyser was operated in fixed analyser transmission (FAT) mode with a pass energy of 50 eV (survey spectrum) and 20 eV (individual peaks). Data analysis was performed on a VGS 5000 data system based on the DEC PDP11 computer. The methodology employed for peak fitting of the peak envelopes has been described in detail [6]. Typically, 1.8–2.0 eV line widths and a Gaussian–Lorentzian mix, with a Lorentzian contribution of 30%, were employed for the components of N1s and Si2p envelopes. Atomic percentage values were calculated from the peak areas using sensitivity factors provided with the data system and background subtraction. The accuracy of the XPS quantitative analysis, as derived for duplicate analyses, was within  $\pm 4\%$ . Spectra were corrected for sample charging by referencing photoelectron peaks to C–C/C–H at 284.9 eV. The precision in the binding energy of the XPS lines, obtained as an average of at least two measurements, was estimated as  $\pm 0.1\ \text{eV}$ .

## 3. Results and discussion

Fig. 1 shows the spectrum of the air-stored silicon nitride powder. The peaks in this spectrum include N1s, Si2p (and Si2s) and O1s core levels and the complementary X-ray induced  $\text{O}_{\text{KLL}}$  and  $\text{N}_{\text{KLL}}$  Auger emissions. All the peaks observed come from the silicon nitride. From observation of an O1s peak and the simultaneous splitting of Si2p and N1s core levels (see below) it can be concluded that some surface oxidation is taking place. Another interesting feature derived from this spectrum is the presence of a very small C1s peak due to ambient contamination. The C1s peak is always present in air-stored samples, unless they are sputtered by a low energy ion beam (typically  $\text{Ar}^+$  ions with an energy of 3–5 keV). The extremely low intensity of the C1s of this sample contrasts with many other reports in the literature, mainly because a carbon-free aluminium cylinder is used in this study as a sample holder.

As known, the binding energy of an element is related to the atomic energy and hence to the electronegativity of the neighbouring atoms. The Pauling electronegativity of the elements involved in  $\text{Si}_3\text{N}_4$  increases in the order  $\text{Si}(1.8) < \text{N}(3.0) < \text{O}(3.5)$ . Thus, the energy of the photoelectron increases when the electronegativity of the neighbouring atom increases. That is, the binding energy of the Si2p peak may change from 99.3 eV for Si(metallic) to 101.4 eV for  $\text{Si}_3\text{N}_4$  and 103.7 eV for  $\text{SiO}_2$ . According to this rule, if more than one species is present on the surface asymmetric peaks would be expected. These effects can be visualized in the Si2p and N1s spectra when recorded under high resolution conditions. Figs 2 and 3 display the Si2p and N1s peaks of an air-stored  $\text{Si}_3\text{N}_4$  powder. These peaks show asymmetrical line profiles that can

TABLE I Characteristics of the starting silicon nitride powder

Main impurities, wt %	C 0.18; O 2.04; Fe < 0.005; Ca < 0.001; Al < 0.005
Specific surface area, $\text{m}^2\ \text{g}^{-1}$	18
Mean particle size, $\mu\text{m}$	0.46
$\text{Si}_3\text{N}_4$ , %	95

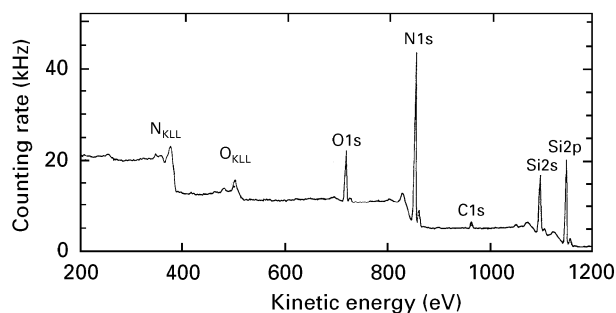


Figure 1 Survey spectrum of the air-stored silicon nitride powder. Two scans were recorded with the analyser operated in the FAT mode at a pass energy of 50 eV. Note the small C1s peak arising from contamination by hydrocarbons.

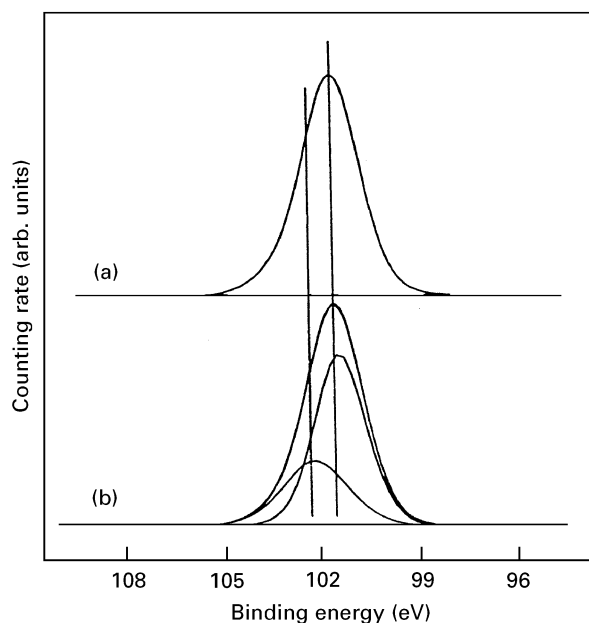


Figure 2 (a) Si2p core level spectrum for the air-stored  $\text{Si}_3\text{N}_4$  powder, (b) The same spectrum after curve fitting to two components (silicon nitride and oxynitride) and S-shaped background removal.

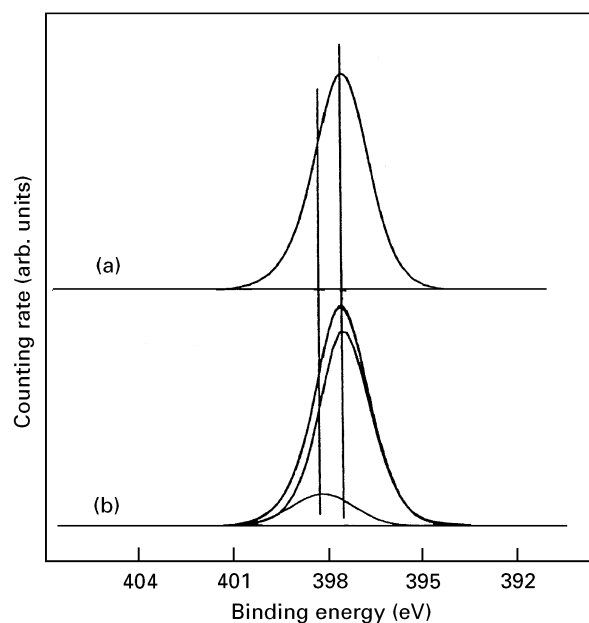
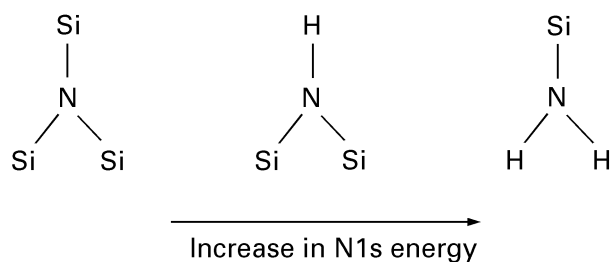


Figure 3 (a) N1s core level spectrum for the air-stored  $\text{Si}_3\text{N}_4$  powder. (b) The same spectrum after curve fitting to two components (nitride and oxynitride) and S-shaped background removal.

TABLE II Binding energies (eV) of core electrons in reference compounds

Compound	Si2p	N1s	O1s	Ref.
$\text{Si}_3\text{N}_4$	$101.1 \pm 0.2$	$397.5 \pm 0.2$	$532.8 \pm 0.2$	[9]
	$102.3 \pm 0.1$	398.3		[8]
	102.2	397.8	532.6	[10]
$\text{Si}_2\text{N}_2\text{O}$	102.1	398.2	534.4	[1]
	101.9	397.9	532.6	[8]
	101.7–102.2	397.3–397.7		[7]
$\text{SiO}_2$	103.6–103.7			[7]
	103.7			[4]

be split into doublets. The full widths at half maxima (FWHM) were found to be 2.0 and 2.1 eV for Si2p and N1s peaks, respectively. Using these FWHMs values, the experimental peaks were calculated and they are displayed in Figs 2b and 3b, respectively. On the basis of binding energy measurements of model compounds [7], the assignment of these peaks to individual species is straightforward. For the silicon oxynitride, the Si2p and N1s binding energies are 101.7–102.2 and 397.3–397.7 eV, respectively (Table II), whereas  $\text{SiO}_2$  gives an Si2p binding energy of 103.4 eV. Accordingly, the low binding energy Si2p (Fig. 2b) and N1s (Fig. 3b) peaks are associated with  $\text{Si}_3\text{N}_4$ . However, the high binding energy of Si2p at 102.6 eV corresponds to an intermediate state between silicon oxynitride (Si2p = 101.9 eV) and silica (Si2p = 103.4 eV), in good agreement with the results of Brow and Pantano [7] and of Bergström and Pugh [8]. Similarly, the high binding energy component of N1s is slightly higher than expected for the silicon oxynitride. This behaviour can be explained as due to a change in the chemical environment of the nitrogen, due to the formation of an amine group [11]. This phenomenon can be represented schematically as



In line with the above reasoning and considering the XPS spectra, it is suggested that the surface region of  $\text{Si}_3\text{N}_4$  powder used in this study has a significant amount of  $\text{Si}_2\text{-NH}$  and  $\text{Si-NH}_2$  groups. In aqueous suspensions, the  $\text{Si}_3\text{N}_4$  surface is populated by  $\text{Si-OH}$  and  $\text{Si}_2\text{-NH}$ . As pointed out by Bergström and Pugh [8], the proportion of these two types of surface groups may be related to the colloidal properties of the silicon nitride particles in suspension. If  $N_B$  is the number of basic amine groups per unit area and  $N_A$  is the number of amphoteric silanol groups per unit area, the ratio  $N_B/N_A$  is directly related to the pH at the isoelectric point. Their results indicate that at  $\text{pH}_{\text{iep}} = 7.9$ ,  $N_B = N_A$ , i.e. the amount of  $\text{Si}_2\text{-NH}$  groups equals that of  $\text{Si-OH}$  groups. Electrophoretic

TABLE III Assignment of the XPS peaks of silicon nitride and surface concentrations of the elements

Peak	Binding energy (eV)	Percentage	Species	Atomic ratio
Si2p	101.6	72	Si <sub>3</sub> N <sub>4</sub>	28
Si2p	102.6	28	SiO <sub>x</sub> N <sub>y</sub>	11
N1s	397.6	80	Si <sub>3</sub> N <sub>4</sub>	41
N1s	398.6	20	SiON(H)	10
O1s	532.7		SiON(H)	

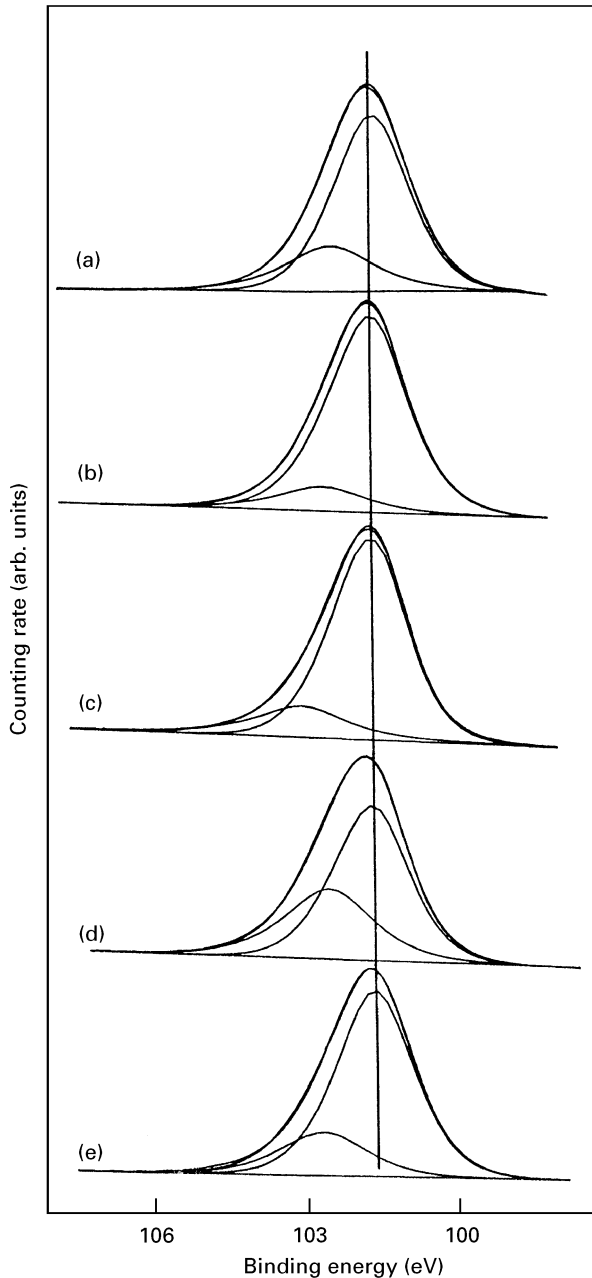


Figure 4 Si2p core level spectra of Si<sub>3</sub>N<sub>4</sub> samples subjected to different processing techniques: (a) slip casting in water, (b) slip casting in isopropyl alcohol, (c) dry isostatic pressing, (d) isostatic pressing in water, and (e) isostatic pressing in isopropyl alcohol. The same experimental methodology as in Figs 2 and 3 was used for quantification.

migration rates on the as-received silicon nitride reveal that its isoelectric points is  $\text{pH}_{\text{iep}} = 8$  [12]. Moreover, the strong smell of ammonia of aqueous suspen-

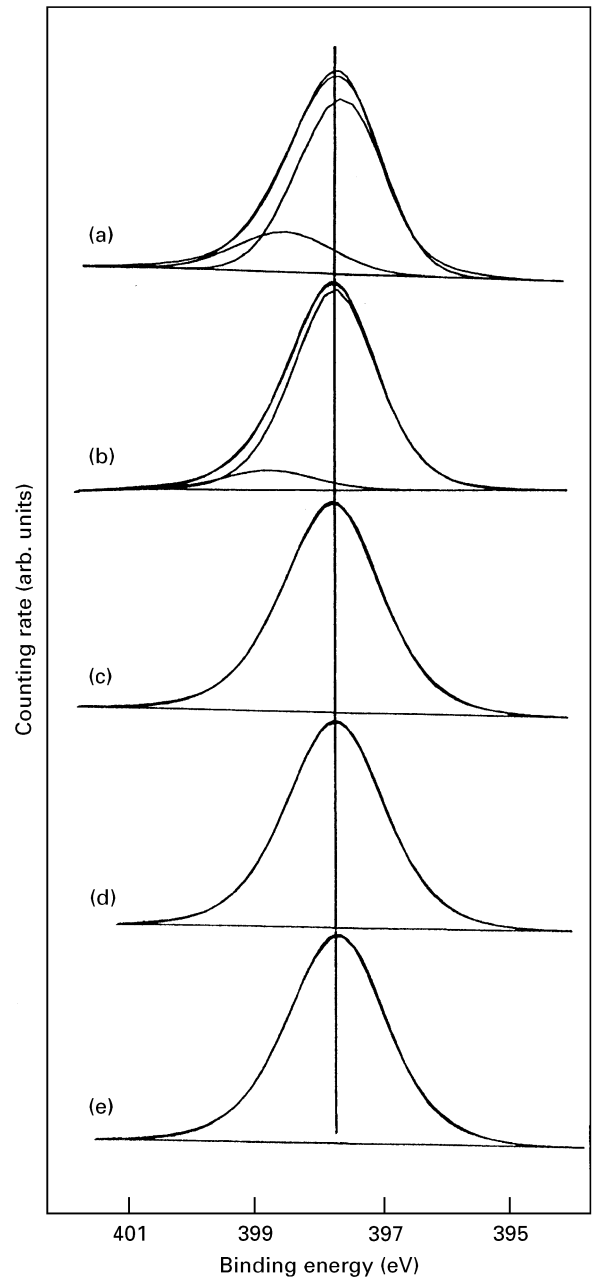


Figure 5 N1s core level spectra of Si<sub>3</sub>N<sub>4</sub> samples subjected to different processing techniques: (a) slip casting in water, (b) slip casting in isopropyl alcohol, (c) dry isostatic pressing, (d) isostatic pressing in water, and (e) isostatic pressing in isopropyl alcohol. The same experimental methodology as in Figs 2 and 3 was used for quantification.

sions is also indicative of hydrolysis phenomena at the surfaces of the powders.

Further insight into the relative abundance of different atoms can be obtained by calculating surface atomic ratios. The atomic concentration,  $C_x$ , of any element,  $x$ , can be calculated by

$$C_x = \frac{I_x/S_x}{\sum_i (I_i/S_i)}$$

where  $I_x$  is the relative peak area of the line spectrum for element  $x$ ,  $S_x$  is the calculated atomic sensitivity factor ( $S_N = 0.45$ ,  $S_{\text{Si}} = 0.27$ ,  $S_O = 0.66$ ) [13]. According to this calculation the N/Si atomic ratio was 1.35 for the as-received powder. Although this value is only slightly higher than the theoretical value (N/Si = 1.33)

TABLE IV Binding energies (eV) of core electrons for silicon nitride samples subjected to different processing conditions

Process	O1s (eV)	N1s (eV) <sup>a</sup>	Si2p (eV) <sup>a</sup>	N/Si	O/Si																																		
Powder Si <sub>3</sub> N <sub>4</sub>	532.7	397.6 (80)	101.6 (72)	1.35	0.28																																		
		398.6 (20)	102.6 (28)			Slipcast In water	532.6	397.5 (82)	101.6 (77)	1.27	0.33	398.3 (18)	102.6 (23)	In alcohol	532.5	397.7 (88)	101.7 (86)	1.39	0.31	398.7 (12)	102.8 (14)	Isostatic pressed	532.7	397.7	101.7 (88)	1.26	0.33	103.2 (12)	101.8 (85)	103.0 (15)	In water	532.6	397.7	101.7 (79)	1.22	0.56	103.0 (21)	In alcohol	532.6
Slipcast In water	532.6	397.5 (82)	101.6 (77)	1.27	0.33																																		
		398.3 (18)	102.6 (23)			In alcohol	532.5	397.7 (88)	101.7 (86)	1.39	0.31	398.7 (12)	102.8 (14)	Isostatic pressed	532.7	397.7	101.7 (88)	1.26	0.33	103.2 (12)	101.8 (85)				103.0 (15)			In water	532.6	397.7	101.7 (79)	1.22	0.56	103.0 (21)	In alcohol	532.6	397.7	103.0 (21)	1.31
In alcohol	532.5	397.7 (88)	101.7 (86)	1.39	0.31																																		
		398.7 (12)	102.8 (14)			Isostatic pressed	532.7	397.7	101.7 (88)	1.26	0.33	103.2 (12)	101.8 (85)				103.0 (15)			In water	532.6	397.7	101.7 (79)	1.22	0.56	103.0 (21)	In alcohol	532.6	397.7	103.0 (21)	1.31	0.34							
Isostatic pressed	532.7	397.7	101.7 (88)	1.26	0.33																																		
			103.2 (12)																																				
			101.8 (85)																																				
			103.0 (15)																																				
In water	532.6	397.7	101.7 (79)	1.22	0.56																																		
			103.0 (21)																																				
In alcohol	532.6	397.7	103.0 (21)	1.31	0.34																																		

<sup>a</sup> Percentages are given in brackets.

for the stoichiometric Si<sub>3</sub>N<sub>4</sub> compound, it suggests, in agreement with the above findings, that a certain population of NH (or NH<sub>2</sub>) groups may well be formed. The assignment of different surface species identified by XPS and their surface concentrations are listed in Table III. From this data it is apparent that 10% of the exposed atoms of the silicon nitride are oxide anions, indicating large oxidation of the material upon exposure to moisture.

Silicon nitride green bodies have been prepared by isostatic pressing and by slip casting in water and in isopropyl alcohol. Figs 4 and 5 show the Si2p and N1s core level spectra, respectively, for all different processing conditions described above. Both binding energies and surface atomic ratios are shown in Table IV. In all cases the O1s spectra display a single peak located at a binding energy of  $532.6 \pm 0.1$  eV, which is close to that of the Si–O bonds. For the samples processed by slip casting, the N1s profile is asymmetric and can be fit to two components at binding energies of 397.6 and 398.6 eV, in complete accordance with that of the starting silicon nitride powder. The exceptions are the isopressed samples that display rather symmetric N1s peaks. In addition, the Si2p peaks (Fig. 4) show larger differences depending on the processing conditions. The binding energy of the higher energy peak shifts towards higher binding energy values in the pressed bodies. The dry powder and bodies obtained by slip casting present initial peaks at  $101.7 \pm 0.1$  eV and second peaks at  $102.7 \pm 0.1$  eV. In the three isopressed samples, prepared by dry mixing and wet mixing in both water and isopropyl alcohol, the higher binding energy Si2p peak contributions appear at a binding energy of  $\geq 103.0$  eV. Although this latter finding indicates, in principle, a deeper oxidation of Si–N bonds in the pressing samples, the O/Si ratios in the last columns in Table IV indicate that the extent of oxidation for the dry and alcohol pressed samples is the same as that observed in the water and alcohol cast samples. The exception is the pressed sample in water, which shows not only the largest surface oxidation but also the

lowest N/Si ratio. Both facts are conclusive that Si–N are strongly altered by moisture.

Slip cast samples have been obtained using TMAH in both water and alcohol, thus affecting the surface characteristics of the Si<sub>3</sub>N<sub>4</sub> powder. The alcohol cast samples present lower O/Si values and higher N/Si values when compared with samples obtained by aqueous slip casting. When the O/Si results of slip casting are compared with those corresponding to isopressed samples, aqueous slip casting seems to give the same extent of oxidation as isostatic pressing after dry mixing or after mixing with alcohol. However, when mixing is done in water very different surface atomic ratios are obtained after pressing, namely as O/Si ratio of 0.562 and a N/Si ratio of 1.217, in contrast with 0.28 and 1.36, respectively, for the starting powder.

In order to check the reliability of the processing conditions with respect to the chemical changes taking place at the Si<sub>3</sub>N<sub>4</sub> surface, simultaneous comparisons of N/Si and O/Si ratios are imperative. For the cast samples, the N/Si and O/Si ratios indicate less oxidized surfaces in the alcohol cast case than in the water cast counterpart, which also agrees with a lower contribution of the high binding energy of the Si2p peak (23% for water cast versus 14% for the alcohol cast sample). Note that this tendency in the percentage of the Si2p peak contribution is not fulfilled for the pressed counterparts; however, the O/Si and N/Si ratios for those samples are in accordance with a larger oxidation in water pressed than in alcohol pressed homologues. It must be mentioned that the quantitative XPS analyses yield a  $\approx 4\%$  uncertainty and the results obtained in this work show slightly higher differences and, hence, it can be stated that there is a tendency that confirms the comments expressed above.

Summarizing, noticeable differences are obtained for samples prepared by water mixing and subsequent isostatic pressing. That is, water clearly affects the surface of the particle, oxidation being strongly enhanced. However, in the case of slip casting in water

this effect does not take place. In practice, formation of  $\text{Si}_3\text{N}_4$  bodies is possible by aqueous slip casting using TMAH as a dispersant. This additive provides a high pH value to the slip, favouring the formation of amino groups at the surface. This fact and the increased nitrogen concentration due to the addition of the dispersant (including this element) promote the formation of a partially oxidized layer that acts as a screen to further oxidation. Still better results can be obtained by using alcohol in the casting, and to a lesser extent in the pressing method. Although the N1s signal was registered it was not detected; then, not more than 0.1% TMAH can remain in the cast green body. The TMAH is a good basic dispersant in slip casting but evaporates during drying, where the double layer disappears and particles consolidate.

#### 4. Conclusions

The influence of various processing routes on the surface chemistry of  $\text{Si}_3\text{N}_4$  has been studied by photoelectron spectroscopy. Surface oxidation has been shown in all cases, but the nature of the oxidized species and the extent of oxidation depend to a large extent on the dispersion media and the route selected for the forming process. Working in high resolution conditions, the Si2p core level spectra were asymmetric, which reveal the presence of intermediate oxidized species. The XPS analyses yield about a  $\approx 4\%$  uncertainty and the results obtained in this work show higher differences and, hence, it can be stated that there is a different tendency to oxidation in the  $\text{Si}_3\text{N}_4$  green compacts obtained by different processing conditions. Surprisingly, the slip casting process yields less oxidized species than with isostatic pressing. This fact may be related to the use of TMAH as a dispersant agent, which stabilizes the suspensions. Due to its chemical character and the resulting high pH value, the formation of amine species at the surface of  $\text{Si}_3\text{N}_4$  during the homogenization steps is also favoured. When working with the casting procedure, TMAH

controls the oxidation because of the formation of a partially oxidized layer around the particles, acting as a screen preventing progressive oxidation.

#### Acknowledgements

This work has been supported by CICYT (Spain) under contract No. MAT94-0741. S. M. Castanho acknowledges RHAEC-CNPq (Brasil) for the concession of a grant.

#### References

1. M. R. PASCUCCI and R. N. KATZ, *Interceram.* **42** (1993) 71.
2. M. H. VAN de VOORDE, C. A. M. SISKENS and W. BETTERIDE, *Sprechsaal* **115** (1992) 1027.
3. K. H. JACK, *J. Mater. Sci.* **11** (1976) 1135.
4. S. I. RAIDER, R. FLITSCH, J. A. ABOAF and W. A. PLISKIN, *J. Electrochem. Soc.: Solid-State Sci. Technol.* **123** (1976) 560.
5. Y. S. JO, J. A. SCHULTZ, S. TACHI, S. CONTARINI and J. W. RABALAIS, *J. Appl. Phys.* **60** (1986) 2564.
6. P. M. H. SHERWOOD, in "Practical surface analysis by auger and X-ray photoelectron spectroscopy", edited by D. Briggs and M. P. Seah (Wiley, Chichester, 1990) pp. 555–86.
7. R. K. BROW and C. G. PANTANO, *J. Amer. Ceram. Soc.* **69** (1986) 314.
8. L. BERGSTRÖM and R. J. PUGH, *ibid.* **72** (1989) 103.
9. M. PEUKERT and P. GREIL, in "Science of ceramics", Vol. 14, edited by D. Taylor (The Institute of Ceramics, Stoke on Trent, UK, 1988) pp. 95–100.
10. M. N. RAHAMAN, Y. BOITEUX and L. C. DE JONGHE, *Bull. Amer. Ceram. Soc.* **65** (1986) 1171.
11. R. K. BROW and C. G. PANTANO, *J. Amer. Ceram. Soc.* **70** (1987) 9.
12. S. R. H. M. CASTANHO and R. MORENO, in Proceeding of Third Euro-Ceramics Conference, Vol. 1, edited by P. Duran and J. F. Fernandez (Faenza Editrice Iberica, Castellón dela Plana, Spain, 1993) pp. 513–18.
13. C. D. WAGNER, L. E. DAVIS, M. V. ZELLER, J. A. TAYLOR, R. H. RAYMOND and L. H. GALE, *Surf. Interface Anal.* **3** (1981) 211.

Received 22 May 1995  
and accepted 17 July 1996